Behavior of optic phonons in the commensurate and incommensurate phases of potassium selenate

Patrick Echegut and François Gervais
Centre de Recherches sur la Physique des Hautes Températures, Centre National de la Recherche Scientifique, 45071 Orléans Cedex 2, France

Nestor E. Massa
Département de Physique et Centre de Recherche en Physique du Solide, Université de Sherbrooke, Sherbrooke, Québec, Canada J1K ZR1

(Received 2 December 1985)

The temperature dependence of infrared reflection spectra of potassium selenate for the three main polarizations is reported for the paraelectric, incommensurate, and ferroelectric phases from 80 to 600 K. Good fits of the factorized form of the dielectric function to reflectivity data were obtained. The number of observed infrared modes are compared with group-theory predictions. In the incommensurate phase, the number of modes is compatible with incipient tripling of the D_{2h}^{16} (*Pnam*) unit cell along the incipient hexagonal **a** axis, according to superspace group-theory predictions. The small dielectric-constant anomaly which occurs at T_I is found to be a consequence of the weak soft-mode-like behavior of some external polar modes. The lock-in transition at T_C is a consequence of an instability of the lattice against the $\mathbf{q}=\mathbf{K}$ polar phason (domain-wall sliding fluctuations), the condensation of which triggers a ferroelectric distortion which abruptly suppresses the incommensurate modulation.

I. INTRODUCTION

Conventional group-theory analysis for prediction of the infrared and Raman activity of lattice-vibration modes is systematically used in the analysis of single-crystal data, in particular when the material undergoes structural phase transitions. However, the problem of the prediction of the number of allowed modes in a *disordered* phase is still open. A way to advance the understanding of this class of phenomena seems to be to study incommensurate phases. Potassium selenate appears to be a good candidate for this purpose because the relative weak damping of most phonon modes in this compound favors the observation of low-energy vibrational modes, and, in particular, the signature of an incommensurate phase, i.e., the amplitude and phason modes. While this compound has been extensively studied by Raman[1-3] and neutron scattering,[4,5] infrared data was still lacking over two-thirds of the frequency range where phonons exist. Furthermore, only two temperatures were investigated and neither corresponded to the incommensurate phase.[6] The present paper reports the temperature dependence of infrared-reflection spectra for the electric field polarized parallel to the three main crystallographic axes of the orthorhombic paraelectric D_{2h}^{16} (*Pnam*) ($Z=4$), incommensurate and ferroelectric C_{2v}^{9} (*Pna*2_1) ($Z=12$) phases of K_2SeO_4 and their analysis. We adopt the notation where **a** represents the incipient hexagonal axis and **c** the polar axis of the ferroelectric phase. Complementary measurements by transmission are also reported. In light of this set of new data, the mechanisms of both commensurate-incommensurate phase transitions will be discussed.

II. SYMMETRIES AND MODE ASSIGNMENTS

Potassium selenate K_2SeO_4 displays the sequence of phases hexagonal D_{6h}^{4} ($P6_3/mmc$) with two molecules per unit cell ($Z=2$) above $T_H=745$ K,[7] orthorhombic paraelectric (PE) with a β-K_2SO_4 prototype structure D_{2h}^{16} (*Pnam*) ($Z=4$),[8] incommensurate (INC) between $T_I=129$ K and $T_C=93$ K with the modulation wave vector at $q_c=(1-\delta)a^*/3$,[4] orthorhombic ferroelectric (FE) C_{2v}^{9} (*Pna*2_1) ($Z=12$).[9] The site symmetry of both potassium atoms and SeO_4^{2-} tetrahedra corresponds to the C_s point group. The factor group analysis complemented by the site method application provides the mode assignments reproduced in Table I. Also in this table are frequencies of internal modes (nonpolar ν_1 and ν_2 and polar ν_3 and ν_4 modes) for the free SeO_4^{2-} ion which has T_d symmetry, in a dilute aqueous solution.

All atoms are in C_1 point-group symmetry in the FE phase. The results of factor group analysis are reproduced in Table II. The A_1, B_1, and B_2 modes are both infrared and Raman active and the number of external and internal modes is detailed in Table III. Note that whereas only 7 B_{1u}, 12 B_{2u}, and 12 B_{3u} are expected in the infrared spectra of the PE phase, 62 modes are expected for each polarization in the FE phase.

Since the symmetry of the incommensurate phase is the average symmetry of the higher-temperature phase, an intuitive point of view might be to expect the same number of modes in both phases. Conversely, de Wolff[10] and Janner and Janssen[11] have shown that the INC phase has a hidden symmetry properly described by superspace groups. Then, application of the superspace group theory to the A_2BX_4 family as developed by Rasing *et al.* for

TABLE I. Correlation table for the orthorhombic PE phase of K_2SeO_4 and related compounds. The frequencies correspond to positions of SeO_4^{2-} internal modes in aqueous solution. The number of additional modes predicted by the superspace group theory (Ref. 12) for the INC phase are in the right column.

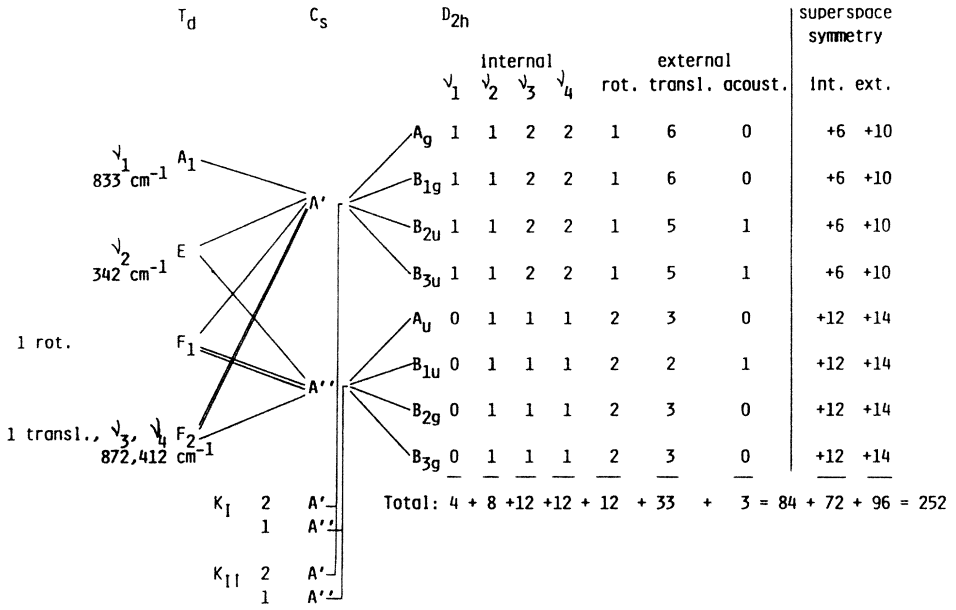

Rb_2ZnBr_4,[12] explicitly gives a number of new infrared hard modes expected in the INC phase. These additional modes are detailed in Table I. Similar predictions have been made by Golovko and Levanyuk[13] and Poulet and Pick.[14] All those theories predict an infinite number of modes in the INC phase. If one restricts oneself, however, to the lowest order, then a finite number is expected. For K_2SeO_4 and isomorphous A_2BX_4 compounds in general, the loss of symmetry related to incommensurability is calculated by considering incipient tripling of the PE-phase unit cell along the **a** modulation axis.

To understand the evolution of spectra on heating in the PE phase, information about the hexagonal phase may be useful. Following the model proposed by Sawada *et al.*[15] for $(NH_4)_2SO_4$ and extended later to K_2SO_4 and K_2SeO_4 by Shiozaki *et al.*,[16] Petzelt *et al.*[6] based their analysis on the following positions for atoms in K_2SeO_4: Se in $2d$ Wyckoff position (D_{3h} point group), K in $2a$ and $2c$, and oxygen in $4f$ and $12k$. In this model called "apex" by Arnold *et al.*[17] for α-K_2SO_4, one apex of SeO_4^{2-} tetrahedron is pointed randomly up or down along the **a** axis, and thus the oxygen sublattice is disordered.

TABLE II. Correlation table for the orthorhombic FE phase of K_2SeO_4.

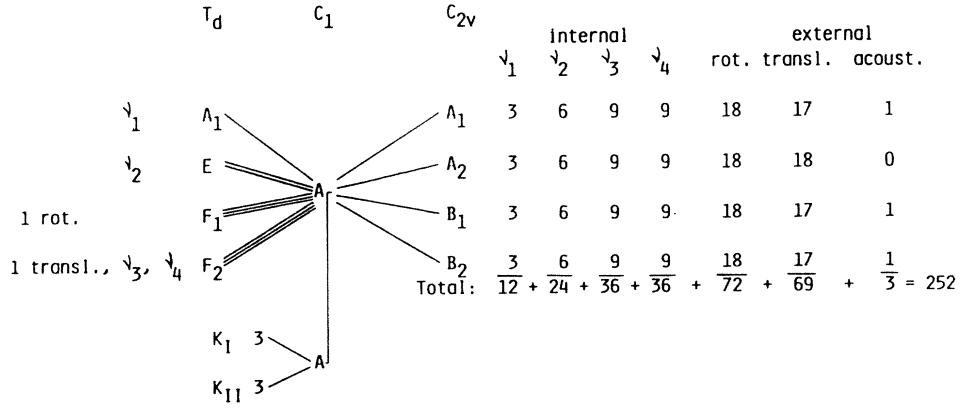

TABLE III. Number of infrared active modes predicted by group theory in the three commensurate phases.

					Internal			
				External	ν_1	ν_2	ν_3	ν_4
Hexagonal	D_{6h}^4	A_{2u}	E||a	2	1	0	1	1
phase	($Z=2$)	E_{1u}	E⊥a	2	0	1	1	1
Orthorhombic	D_{2h}^{16}	B_{1u}	E||c	4	0	1	1	1
paraelectric	($Z=4$)	B_{2u}	E||b	6	1	1	2	2
phase		B_{3u}	E||a	6	1	1	2	2
Orthorhombic	C_{2v}^9	A_1	E||c	35	3	6	9	9
ferroelectric	($Z=12$)	B_1	E||a	35	3	6	9	9
phase		B_2	E||b	35	3	6	9	9

The factor group analysis of Petzelt *et al.*[6] is performed with C_{3v} site symmetry for the SeO_4^{2-} tetrahedron, which represents an average symmetry of both types of SeO_4^{2-} sites. Results are reproduced in Table III for infrared-active A_{2u} and E_{1u} modes. The application of group theory to a disordered system is obviously questionable and the present case constitutes a further test related to the general question raised in this paper that we attempt to answer by an experimental approach.

III. EXPERIMENTAL PROCEDURE AND DATA ANALYSIS

A. Experimental

Potassium selenate single crystals were grown by isothermal slow evaporation from aqueous solution. Some samples were grown at room temperature, whereas some others were grown at 40 °C by G. Hauret now at Centre de Recherches sur la Physique des Hautes Températures. Crystalline plates were cut parallel to crystallographic axes and polished. Infrared reflectivity measurements were performed with a rapid-scan Fourier spectrometer Bruker IFS 113 described elsewhere.[18] Spectra for the electric field polarized along **a** (B_{3u} spectrum), **b** (B_{2u}), and **c** axes (B_{1u}) were recorded over the temperature range 80–600 K. A partial alteration of the crystal occurs above 600 K and prevented us from reaching the hexagonal phase. Arnold *et al.*[17] have shown that, in potassium sulfate, smaller crystals burst into pieces at about the same temperature. They verified that the growth of small bubbles makes the crystal explode when vapor pressure is high enough and proposed the following exothermic reaction

$$[K_{1-x}(OH_3)_x]_2SO_4 \xrightarrow{570\ K} (K_{1-x}H_x)_2SO_4 + 2xH_2O\uparrow, \quad x \ll 1 .$$

A recombination of hydrogens occurs at higher temperature. The same phenomenon has been verified by Unruh *et al.*[19] in potassium selenate. It correlates well with the appearance of peaks in differential thermal analysis in the 375–745 K region as well as with the defect-induced structure that appears in Raman spectra.[3] Note, however, that infrared transmission spectra, well known to be very sensitive to OH stretching vibrations, did not reveal hydroxil traces.

Results for the three successive PE, INC, and FE phases covering the frequency range from 20 to 1000 cm^{-1} are shown in Fig. 1. No reflection band is observed above 1000 cm^{-1}. The low-frequency region below 400 cm^{-1} had been investigated previously[6] at 90 and 300 K only. Excellent agreement is found between both sets of external mode spectra (below 250 cm^{-1}). However, significant disagreements are found in the ν_4 internal mode region. Deformations of band profiles in spectra of Ref. 6 are supposed to be caused by the small transmission of the beamsplitter and/or phase errors in this spectral region which constitutes the upper limit of the kind of instrument utilized in Ref. 6. Besides, spurious bands near 350 cm^{-1} were interpreted as ν_2 modes. In fact, these features are local increases of signal due to the partial transmission through their thin sample with decreasing temperature and additional reflection upon the back surface. There is actually no reflection band in this region, but transmission measurements through a 720-μm-thick sample reveal ν_2 modes (Fig. 2) with oscillator strengths indeed much too weak to give rise to reflection bands.

The static dielectric constant ϵ_0 is straightforwardly deduced from the extrapolation of the low-frequency reflection level—which, in practice, is nearly flat—to zero frequency, via the relationship

$$(\epsilon_0)^{1/2} = \left[\frac{1+(R_0)^{1/2}}{1-(R_0)^{1/2}} \right] . \tag{1}$$

Results are in agreement with the values obtained by macroscopic measurements,[20] except for the dielectric anomaly observed at T_C along the polar axis. This important point will be discussed later on.

B. Analysis

A computer simulation of experimental spectra is also shown in Fig. 1. This is achieved with the aid of the factorized form of the dielectric function[18]

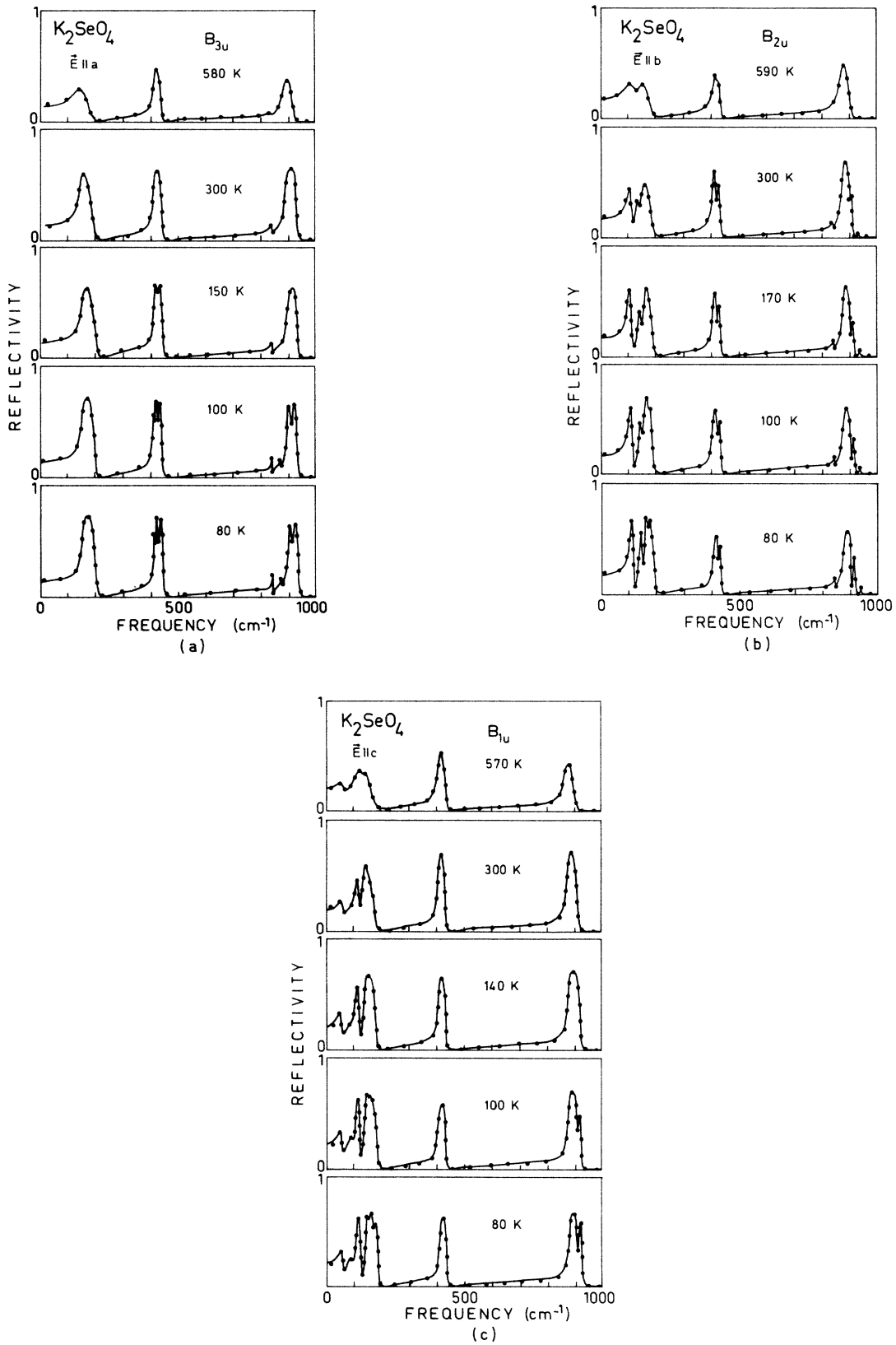

FIG. 1. Temperature dependence of reflection spectra over the three phases (PF,INC,FE) for the electric field polarized parallel to the three axes: (a) **E**||**a**, (b) **E**||**b**, and (c) **E**||**c**. Dots are experimental data and the solid line is the best fit of the factorized form of the dielectric function.

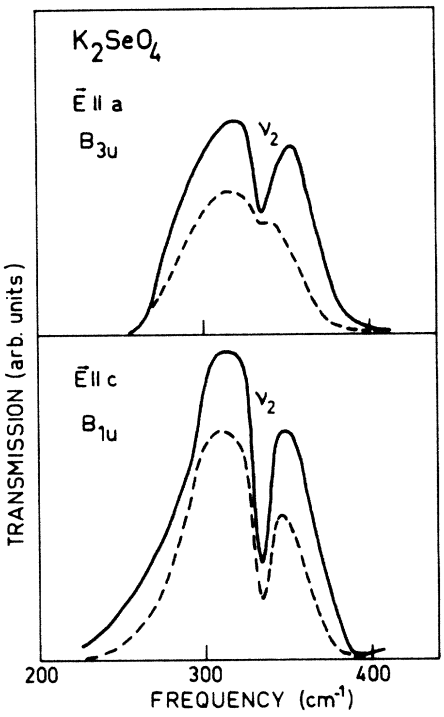

FIG. 2. Transmission spectrum in ν_2-mode region for **E**||**a** and **E**||**c** for two temperatures: $T=300$ K (dashed lines) and $T=80$ K (solid lines).

$$\epsilon=\epsilon_\infty \prod_j \left[\frac{\Omega_{jLO}^2-\omega^2+i\omega\gamma_{jLO}}{\Omega_{jTO}^2-\omega^2+i\omega\gamma_{jTO}} \right], \tag{2}$$

where the Ω_j's and γ_j's represent the frequencies and dampings of transverse (TO) and longitudinal optical (LO) modes, respectively. ϵ_∞ is the high-frequency dielectric constant. From the parameters which give rise to the best fit to experimental reflection spectra, the oscillator strengths of the polar TO modes—that are not fit parameters in this model—are deduced from the TO-LO splittings via the relationship

$$\Delta\epsilon_j=\epsilon_\infty \Omega_{jTO}^{-2} \frac{\prod_k (\Omega_{kLO}^2-\Omega_{jTO}^2)}{\prod_{k\,(\neq j)} (\Omega_{kTO}^2-\Omega_{jTO}^2)} . \tag{3}$$

Similarly, the strengths of LO modes are deduced from the relation

$$\Delta\eta_j=\frac{1}{\epsilon_\infty}\Omega_{jLO}^{-2} \frac{\prod_k (\Omega_{kTO}^2-\Omega_{jLO}^2)}{\prod_{k\,(\neq j)} (\Omega_{kLO}^2-\Omega_{jLO}^2)} . \tag{4}$$

The temperature dependence of TO- and LO-phonon responses, which correspond to the imaginary parts of the dielectric and inverse dielectric functions, respectively, is displayed in Fig. 3 for the electric field polarized along the three main directions.

Since TO-LO splittings are due to the Coulombic field, effective charges may be straightforwardly deduced via a generalization of a relation of the form

$$\Omega_{LO}^2-\Omega_{TO}^2=\frac{(Ze)^2}{\epsilon_v V} \tag{5}$$

which holds for cubic diatomic crystals, and is written as[21,22]

$$\sum_j (\Omega_{jLO}^2-\Omega_{jTO}^2)_\alpha=\frac{1}{\epsilon_v V}\sum_k \frac{(Ze)_{k\alpha}^2}{m_k} , \tag{6}$$

where V is the volume occupied by the k ions of mass m_k, α is the direction of polarization, and ϵ_v is the dielectric constant of vacuum. Taking account of the electric neutrality, two equations are available to solve a system with three unknowns in the case of ternary compounds. However, when the description in terms of internal and external vibration modes holds and when there is no significant coupling between both types of modes, the problem may be solved by considering the relative motions of molecular ion vibrating against external cations, and summing over external modes only on the left-hand side of Eq. (6).

IV. RESULTS AND DISCUSSION

A. Frequencies and vibrational mode assignment

Three distinct spectral regions are clearly visible in Figs. 1 and 3. External modes (translational and librational vibrations) lie in the range 20–250 cm^{-1}. ν_3 and ν_4 modes form two well-separated characteristic groups around 900 and 420 cm^{-1}, respectively. ν_1 modes are observed at $\simeq$840 cm^{-1}. As mentioned above, transmission measurements in the 250–400 cm^{-1} window reveal ν_2 modes (Fig. 2). Note that observed internal TO mode frequencies also very close to those of the selenate radical in solution, that makes assignments straightforward.

If we omit lowest-frequency external modes of the B_{1u} spectrum, the number of modes in the highest-temperature spectra is already that expected for the upper hexagonal phase. This is true several hundred degrees below the phase transition temperature. On cooling in the D_{2h}^{16} phase, the full number of expected internal modes becomes observed in the B_{2u} and B_{3u} spectra while the number of observed B_{1u} modes remains the same as that of E_{1u} representation as predicted theoretically (Table III). Additional external modes are observed in the PE phase for the three polarizations. Their number is however less than expected from group theory. TO and LO frequencies in the B_{3u} spectrum, which corresponds to the incipient hexagonal axis, are significantly higher than in the other two polarizations. Main modes are similar for both axes perpendicular to the **a** axis. The evolution of spectra on heating in the PE phase and positions and widths of main lines are fully consistent with a small distortion of the higher-temperature hexagonal structure. This pseudohexagonal character is further confirmed by

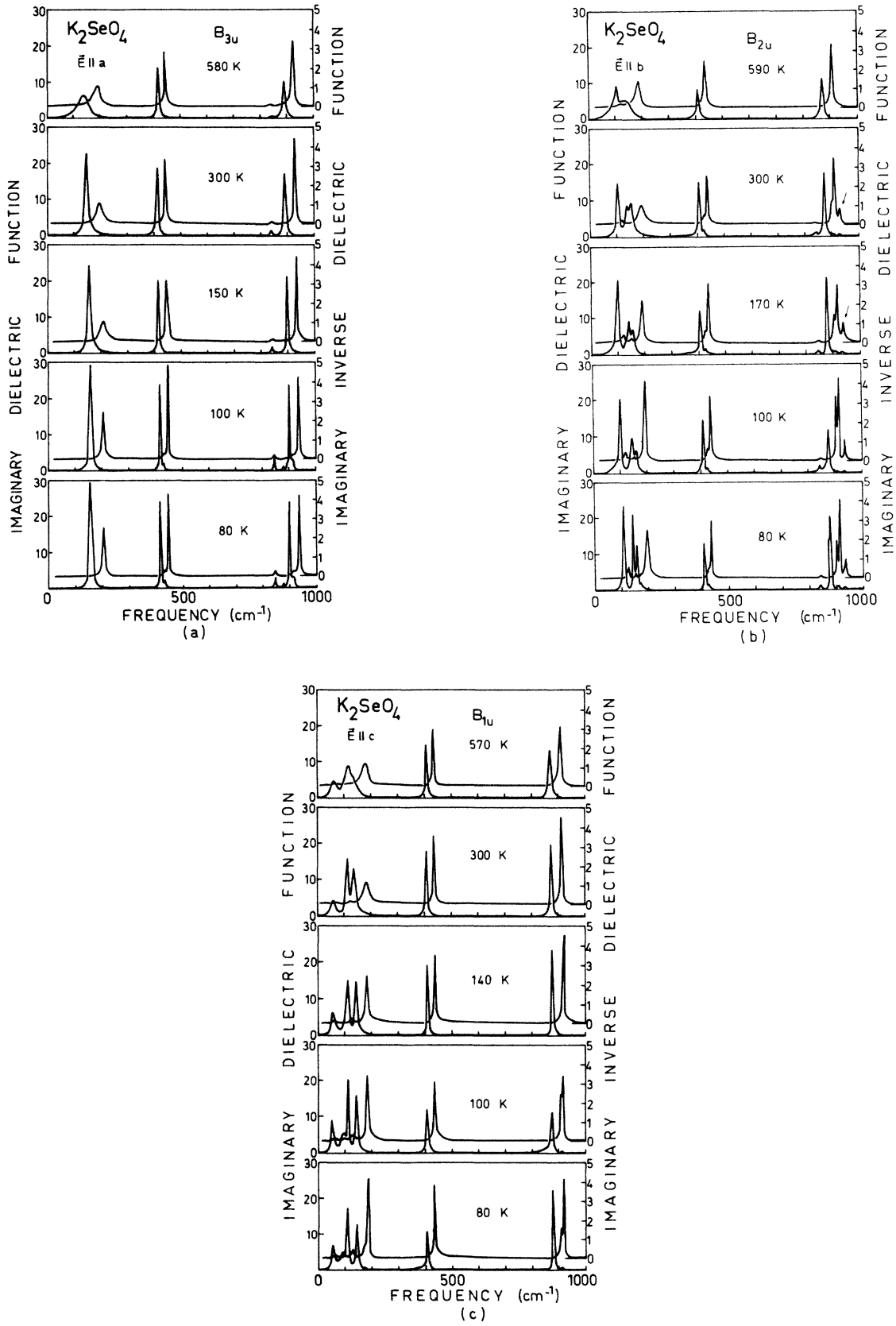

FIG. 3. Infrared response of transverse optical (TO, imaginary dielectric function) and longitudinal optical (LO, imaginary inverse dielectric function) phonons for the electric field polarized parallel to the three axes: (a) **E**||**a**, (b) **E**||**b**, and (c) **E**||**c**.

the analysis of main internal Raman frequencies.[2] Summarizing, potassium selenate presents no anomaly when experiment is compared with group-theory predictions. We have to point out however that some samples which probably contained extrinsic defects displayed a weak additional ν_3-mode symmetry forbidden in the B_{2u} spectrum (denoted by an arrow in Fig. 3). On the other hand, Raman scattering cross section corresponding to the A_g spectrum—in particular the symmetric stretching modes—is found much stronger than at any other polarizations, particularly $\ldots(ba)\ldots$ configuration.[2] This implies weaker correlations of internal vibrations perpendicular to the **c** axis. In other words, the phonon energy is dependent upon wave vector in the c^* direction, due to the local electric field induced by the D_{2h}^{16} structure, whereas phonon branches would be flatter (molecular vibrations) perpendicular to it. The weakness of correlations of internal vibrations in the (ab) plane favors a small (infrared and Raman) activity of forbidden modes, the effect being enhanced by extrinsic defects.

When samples are cooled in the INC and FE phases, a number of new modes (Fig. 4) become infrared active just below T_I. These additional modes appear for the three polarizations and each vibration group—external, internal—is concerned. No change in the number of observed modes is observed at the INC-COM (where COM represents commensurate) phase transition at 93 K and there is only continuation of phenomena related to the second-order phase transition at $T_I = 129$ K. A possible exception to this rule is noticed in a particular Raman-active phonon at about 75 cm^{-1}, $\ldots(aa)\ldots$, also observed in Ref. 19. At room temperature, this mode has an asymmetrical line shape that persists into the INC phase to only break down at the onset of the soliton lattice ($T \simeq 110$ K) where it develops side bands on the higher-frequency side. At 27 K, the spectrum clearly resembles the effect expected by a triple folded Brillouin zone (Fig. 5). Those FE-phase-allowed modes are observed in the INC phase at least up to $\simeq 110$ K.

The number of additional infrared modes for $\mathbf{E}||\mathbf{c}$, viz., $1\nu_3 + 1\nu_4$ and 2 external, observed in the INC phase, appears compatible with the application of the superspace theory[12] to the case of A_2BX_4-type crystals (Table I). This number remains the same in the orthorhombic FE phase and is much smaller than that predicted by group-theoretical analysis in spite of the loss of inversion center associated with the appearance of ferroelectricity. Moreover, systematic simultaneous infrared *and* Raman activity for all A_1, B_1, and B_2 modes is not observed contrary to group-theory predictions for the C_{2v}^9 FE phase.

The temperature dependence of the TO and LO frequencies of all modes is plotted in Fig. 6. In the immediate vicinity of the phase transitions, small frequency shifts occur, likely induced by atomic rearrangements. On the other hand, most of mode frequencies linearly decrease on heating in the PE phase. This behavior results from the balance of two effects, (i) the anharmonic phonon coupling contribution to the phonon self-energy and (ii) the influence of lattice thermal expansion. If three phonon couplings only are retained and if a positive mode Grüneisen parameter is considered, then both contributions have the same sign and a downshift of frequencies is consistently observed. Contrary to this common behavior, a few low-frequency external modes exhibit an upshift with increasing temperature. Such a phenomenon has a Raman counterpart in two excitations that, a few degrees above T_I, seem to merge into one (Fig. 7). They are best seen in a 45° scattering geometry for phonon propagation along the principal orthorhombic axes, and they are probably related to librational motions. To explain this soft-mode-like behavior, one may invoke either a fourth-order anharmonic quartic potential and/or a negative mode Grüneisen parameter, more specifically, anharmonic coupling with the soft mode. The study of the pressure dependence of those frequencies would help to draw conclusions regarding the dominant contribution. For infrared modes polarized along the polar **c** axis, the combination of such effects over all modes explains the small dielectric constant anomaly near T_I.

Amplitude and phason modes are expected in the low-frequency region. Petzelt[23] predicts the infrared activity of $q = K$ amplitude and phason modes for $\mathbf{E}||\mathbf{c}$ in the INC phase, $q = 0$ amplitude mode for $\mathbf{E}||\mathbf{c}$, and $q = 0$ phason for $\mathbf{E}||\mathbf{a}$ in the FE phase, but with so small oscillator strengths that the chances to observe them are little. No mode is observed in our reflection spectra in the expected frequency range. More specifically, the low-frequency reflection level for $\mathbf{E}||\mathbf{c}$ exhibits such small dependence on temperature that it cannot account, by any means, for the dielectric constant anomaly around T_C. Transmission spectra for $\mathbf{E}||\mathbf{a}$ do not reveal any structure below 100 cm^{-1} in the FE phase which is not really surprising since no extra mode characteristic of the FE distortion has been experimentally observed in the spectrum. For $\mathbf{E}||\mathbf{c}$, our 720-μm-thick sample totally absorbed infrared radiation below 50 cm^{-1} in the vicinity of T_C, whereas it partially transmits at higher and lower temperature. We infer this absorption to the high-frequency edge of the $q = K$ phason, which would have a frequency well below the range available to our spectrometer and an oscillator strength large enough to fit the dielectric constant anomaly, in agreement with the interpretation of millimeter wave measurements of Petzelt *et al.*[6] Note that the frequency of the domain wall sliding fluctuation ($q = K$ phason) was found to shift from 0.7 cm^{-1} at 104 K down to 0.06 cm^{-1} at 95 K. The amplitude mode is not observed at 80 K in our transmission spectra and could be merged in the low-frequency edge of the 50 cm^{-1} mode. It is not expected however to play any role in the transition at T_C.

B. Raman scattering cross sections and infrared mode line shapes

The temperature dependence of TO and LO dampings of main modes of each vibrational group is displayed in Fig. 8. Two kinds of behaviors are observed in the PE phase. Internal mode dampings show a linear increase upon heating ascribed to cubic anharmonicity. On the other hand, main LO ($\simeq 180$ cm^{-1}) external mode dampings show anomalous evolution with temperature in the PE phase. Normally, the temperature dependence of

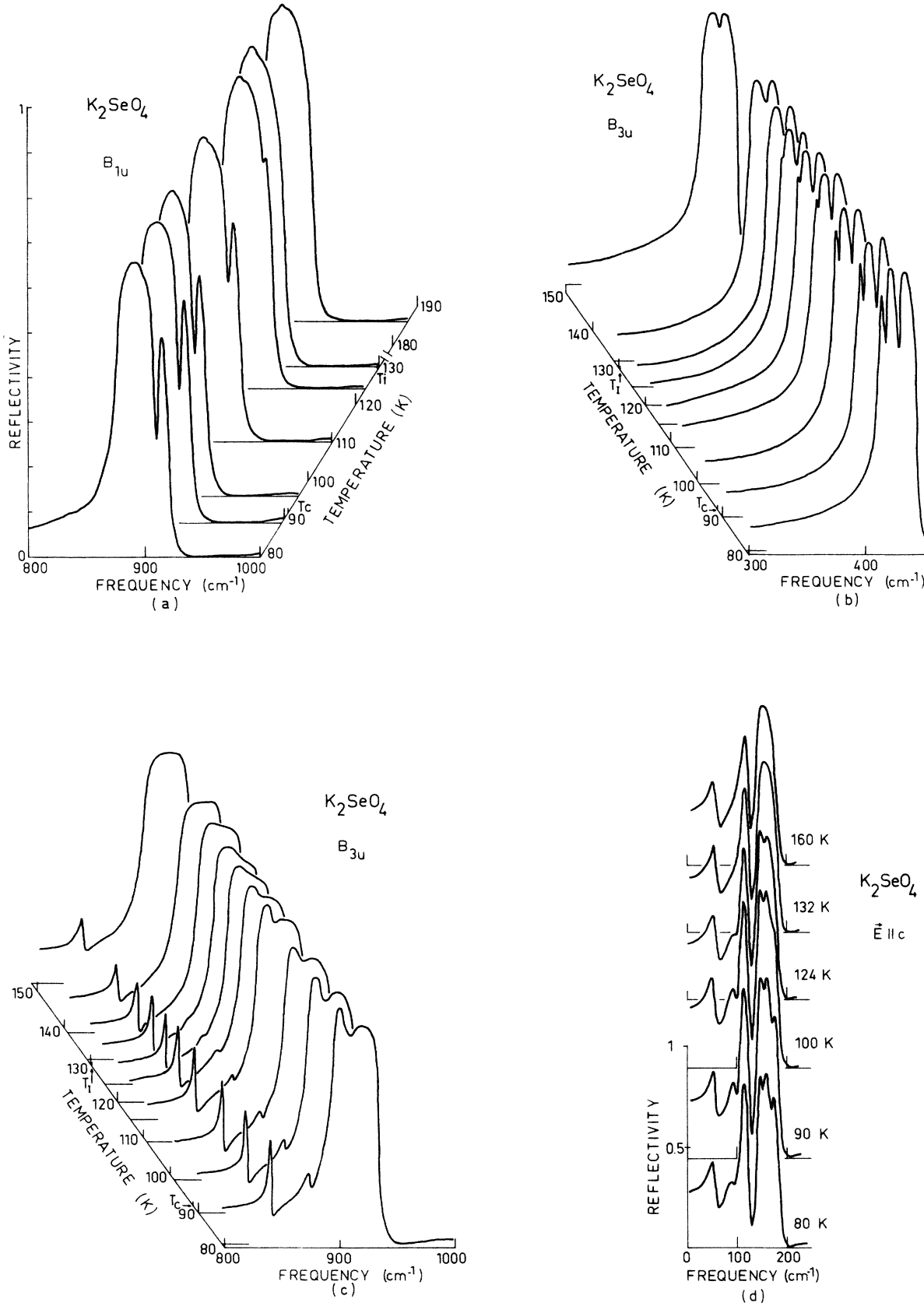

FIG. 4. Temperature dependence of infrared reflectivity: (a) in the ν_3-mode region for **E**||**a**; (b) in the ν_2-mode region for **E**||**c**; (c) in the ν_1- and ν_3-mode region for **E**||**c**; (d) in the external-mode region for **E**||**c**.

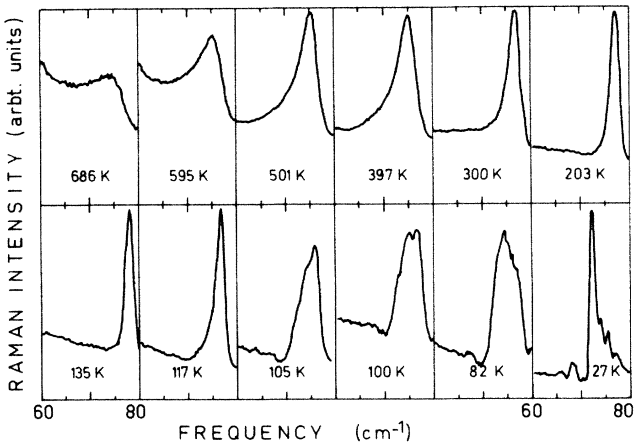

FIG. 5. Temperature dependence of the A_g Raman-active resonantlike feature in the (60—80)-cm^{-1} region of the ...(*aa*)... scattering configuration (see also Ref. 2).

mode dampings obey a law of the form

$$n(\omega/2)+\tfrac{1}{2}\ ,$$

where (7)

$$n(\omega/2)=[\exp(h\omega/2k_BT)-1]^{-1}$$

is the mean number of phonons (dotted lines in Fig. 8). Anomalous line broadening superimposed over the $n(\omega/2)+\frac{1}{2}$ contribution is observed above T_I for these LO modes. Note that the anomaly appears maximum around 250 K. A related phenomenon was observed in Raman measurements in the highest-intensity group of external phonons. We already pointed out[24] the possible correlation with phonon-assisted optical transitions as determined from the measurements of the temperature dependence of the absorption edge. Specifically, the highest-intensity lattice Raman frequencies coincide with phonon frequencies entered as fitting parameters in the Urbach's rule formalism.[25] The anomalous LO mode dampings shown in Fig. 8 may be also thought of as a consequence of this mechanism, again because these modes have frequencies and symmetries consistent with the vibrational groups involved in Urbach's fitting. Note that 250 K is indeed the temperature at which the Σ_2,Σ_3, c polarized, extended branch begins its most pronounced softening.[4] On the other hand, geometry-dependent Raman scattering cross sections are found for the internal vibrations at any temperature.[26] Figures 9(a) and 9(b) show the spectra in the PE phase for 90° Raman configuration (see inset of Fig. 7) in the bending and stretching regions. This is to be compared against those for phonons propagating along one of the crystal principal axes (solid curves). A clear reversal in intensity is observed for each vibrational group. This effect is particularly striking for the ν_1 (A_{1g}) mode, 840 cm^{-1}, a feature that is by far dominant. Consequently, a proper interpretation is that the SeO_4^{2-} sublattice is interacting with the crystal field as a whole polarizable anion. Such an effect has no infrared counterpart, pointing again to the electronic intermediate Raman states. Such a suggestion is to be compared with the approach of Bilz and co-workers[27] which emphasizes the leading role played by the nonlinear strong oxygen polarizability in the electron-phonon interactions thought to be the origin of mode softening.

C. Effective charges

Following the discussion of Sec. III B, effective charges of such a ternary compound may be evaluated since external and internal mode regions do not overlap. In a first step, we consider the vibrations of potassium ions against SeO_4^{2-} molecular ions, and sum over external modes only so that Eq. (6) is rewritten as

$$\sum_j(\Omega^2_{j\mathrm{LO}}-\Omega^2_{j\mathrm{TO}})_\alpha=\frac{1}{\epsilon_v V}\sum_{k_1,k_2}\left[\frac{(Z_{\mathrm{K}}e)^2_{k_1}}{m_{\mathrm{K}}}+\frac{(Z_{\mathrm{SeO_4}})^2_{k_2}}{m_{\mathrm{SeO_4}}}\right]. \tag{8}$$

From (8) combined with the electric neutrality condition, the effective charge of K is deduced straightforwardly. Then we consider all modes and make use of (6)

$$\sum_{j'}(\Omega^2_{j'\mathrm{LO}}-\Omega^2_{j'\mathrm{TO}})_\alpha=\frac{1}{\epsilon_v V}\sum_{k_1,k_2,k_3}\left[\frac{(Z_{\mathrm{K}}e)^2_{k_1}}{m_{\mathrm{K}}}+\frac{(Z_{\mathrm{Se}}e)^2_{k_2}}{m_{\mathrm{Se}}}+\frac{(Z_{\mathrm{Ox}}e)^2_{k_3}}{m_{\mathrm{Ox}}}\right], \tag{9}$$

where Z_{K} is already known from the former step, combined with the electric neutrality. Therefore,

$$\sum_{k_1,k_2,k_3}[(Z_{\mathrm{K}})_{k_1}+(Z_{\mathrm{Se}})_{k_2}+(Z_{\mathrm{Ox}})_{k_3}]=0\ . \tag{10}$$

From the system of Eqs. (9) and (10), the three effective charges are deduced over the whole temperature range. No significant dependence of each charge is found either on temperature or polarization. Results are $Z_{\mathrm{K}}=0.75$, $Z_{\mathrm{Se}}=2$ (reduced effective charge $Z/Z_{\mathrm{O}}=0.33$), and $Z_{\mathrm{Ox}}=0.9$ ($Z/Z_{\mathrm{O}}=0.45$). The low effective charge of selenium is consistent with the almost covalent bonding within the SeO_4^{2-} molecular group. The fact that such effective charge values are averaged over different sites might explain why they are insensitive to the phase transitions, at least their antiferrodistortive components. Nevertheless, results are consistent with the pseudoisotropic nature of the SeO_4^{2-} surrounding, and tetrahedra rotations below T_I do not significantly alter this pseudosymmetry.

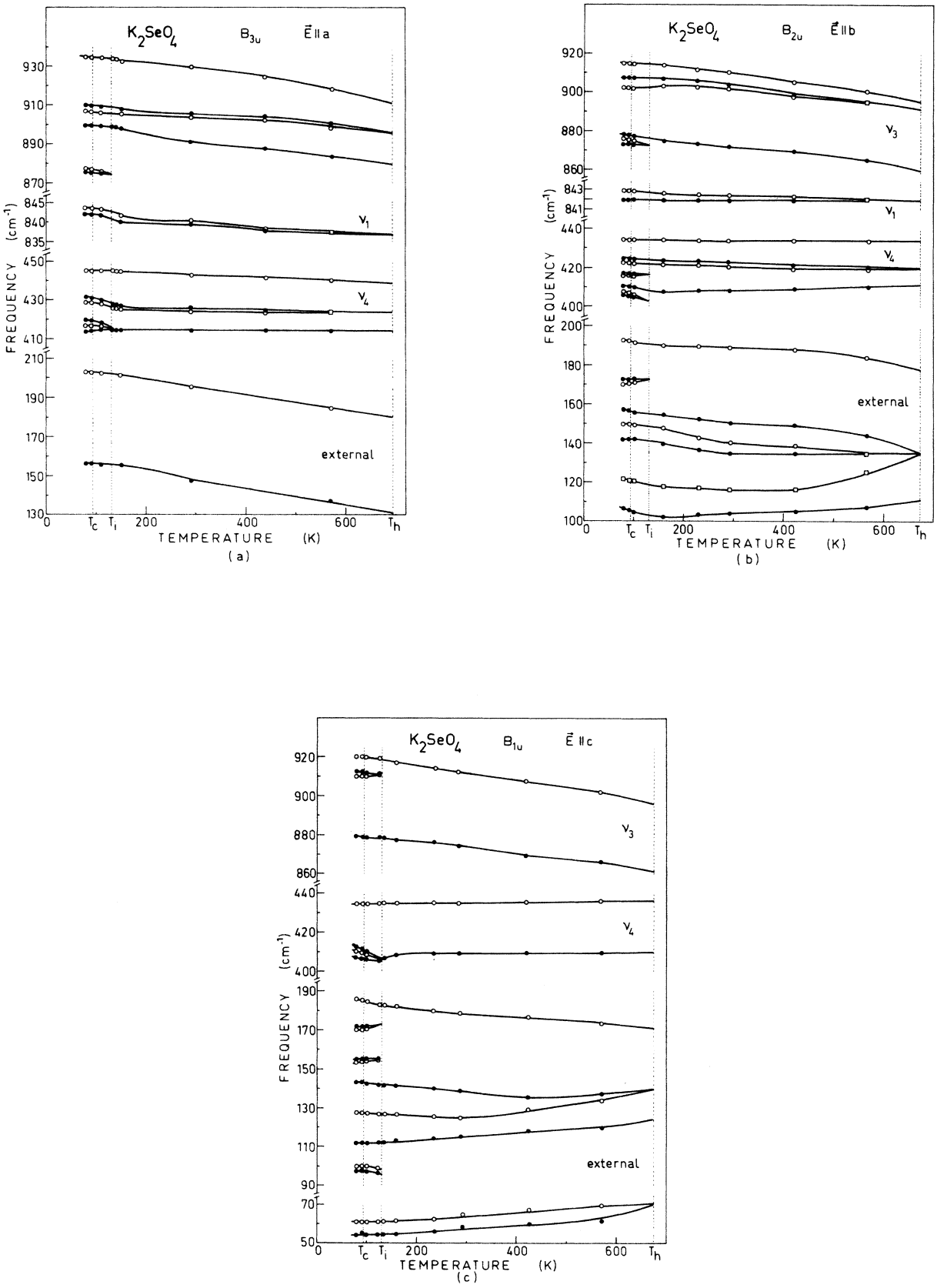

FIG. 6. Temperature dependence of TO (●) and LO (○) phonon frequencies for (a) E||a, (b) E||b, and (c) E||c. Solid lines are guides to eye.

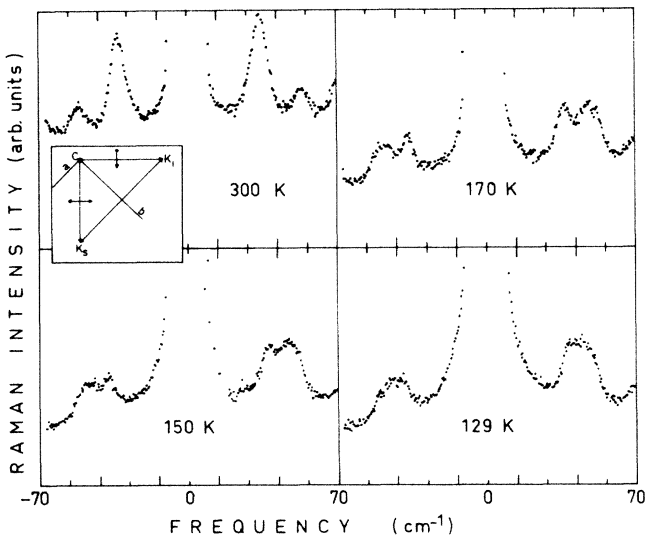

FIG. 7. Temperature dependence of Stokes and anti-Stokes components of the lower-frequency spectra of K_2SeO_4 taken for phonon propagation along the **a** orthorhombic axis.

D. Oscillator strengths

The oscillator strengths of all polar modes do not depend on temperature in the PE phase, except for the ν_1 mode in the B_{3u} spectrum. Its evolution is displayed in Fig. 10 and is fitted by a power law $(T_H - T)^{1.4}$. As mentioned in Sec. II, the relative intensity decrease on heating in the PE phase is reminiscent of the upper phase transition. Potassium selenate is isostructural with α- and β-K_2SO_4. For the hexagonal phase, three space groups D_{3d}^3,[28] C_{6v}^4,[29] and D_{6h}^4,[16] have been proposed during the last decade. The D_{6h}^4 space group is commonly accepted to explain the crystal structure of K_2SeO_4 by analogy to α-K_2SO_4. The D_{6h}^4 model suggested by Shiozaki *et al.*[16] is such that, in the orthorhombic phase, SeO_4^{2-} (or SO_4^{2-}) radicals have two stable states (up and down), and the orthorhombic-hexagonal phase transition corresponds to a disorder over both possible configurations. Arnold *et al.*[17] suggest an additional model for the vicinity of the phase transition below the "apex" regime. In their "edge" model, one edge of tetrahedron is parallel to the **a** axis and three SO_4^{2-} groups are statistically superimposed. A Raman study by Ishigame *et al.*[30] shows that external modes are compatible with the D_{6h}^4 group, but, to overcome some difficulties related to the orientational disorder of tetrahedra, they suggest that a correlation between directions of two SO_4^{2-} ions exists locally in the unit cell of the hexagonal phase. Arnold *et al.*[31] have found that a longitudinal-acoustic (LA) mode, characteristic of the flipping of the SO_4^{2-} tetrahedra, becomes soft along the hexagonal **a** axis.

Figure 11 shows the temperature dependence of the oscillator strengths of the additional modes in the INC and FE phases. Only the best-resolved mode strengths are plotted. No detectable discontinuity in their temperature dependence is observed at T_C, and no change of slope is found in the investigated temperature range. Those phenomena are confirmed by similar studies of K_2ZnCl_4 and Rb_2ZnCl_4,[32] for which the available temperature range is wider, especially in the FE phase. Data are reproduced in Fig. 11. Oscillator strengths of new modes below T_I obey power laws of the form $(T_I - T)^x$. The common slope in the log-log scale is $x=1$ for **E**||**a** and $x=0.75$ for **E**||**c**. The latest value compares well with that obtained for the temperature dependence of the $q=0$ Raman amplitude mode intensity also plotted in Fig. 11. The additional modes observed for **E**||**b** are too weak to deduce an exponent. This behavior, therefore, appears to be general to A_2BX_4 compounds. On the other hand, $x=0.75$ for **E**||**c** and $x=1$ for **E**||**a** agree with exponents deduced from lattice thermal expansion measurements,[33] and the evolution of several other physical quantities.[23] Besides, if one admits that the conclusions of theoretical approaches valid in the $T=T_I$ limit may be extrapolated to lower temperatures, this "critical" exponent 0.75 agrees with experimental data obtained by Majkrzak *et al.*[34] and compares well with the predictions of a XY model of ferromagnetism.

V. SYMMETRY AND INFRARED ACTIVITY IN THE INC PHASE

Present measurements show that the PE-INC phase transition is characterized by the appearance of vibrational hard modes forbidden by symmetry in the D_{2h}^{16} PE phase, (i) the number of which is compatible with the incipient tripling of the unit cell, but (ii) remaining much smaller than that expected in the FE phase, and (iii) no new mode appears on further cooling at T_C. All this information wholly confirmed in our studies of potassium and rubidium zinc chloride, allows us to assert that the effective symmetry of the incommensurate phase, as seen from infrared spectroscopy, corresponds to a tripling of D_{2h}^{16} along the **a** direction neglecting the deviation δ to the commensurate wave vector $q_c = a^*/3$. The fact that no detectable change of power exponents x was found in the INC phase, irrespective of plane-wave or soliton regimes, and then in the commensurate FE phase, should be emphasized. This is in perfect agreement with the application of superspace group to the case of A_2BX_4 compounds, or Landau approaches as well.

VI. INC-COM PHASE TRANSITION

On cooling in the INC phase, there is growing of domains with commensurate structure and spontaneous polarizations of opposite signs which are separated by discommensuration regions (soliton regime where the phase is a nonlinear function). There is a decrease of the soliton density, increase of the intersoliton distance and, therefore, growing in the coherence of domain wall sliding fluctuations on cooling towards T_C. At this temperature, probably because the intersoliton distance exceeds some critical value, the condensation of correlated domain wall fluctuations along **a**, triggers a ferroelectric distortion, simply because the component along **c** is nothing but the

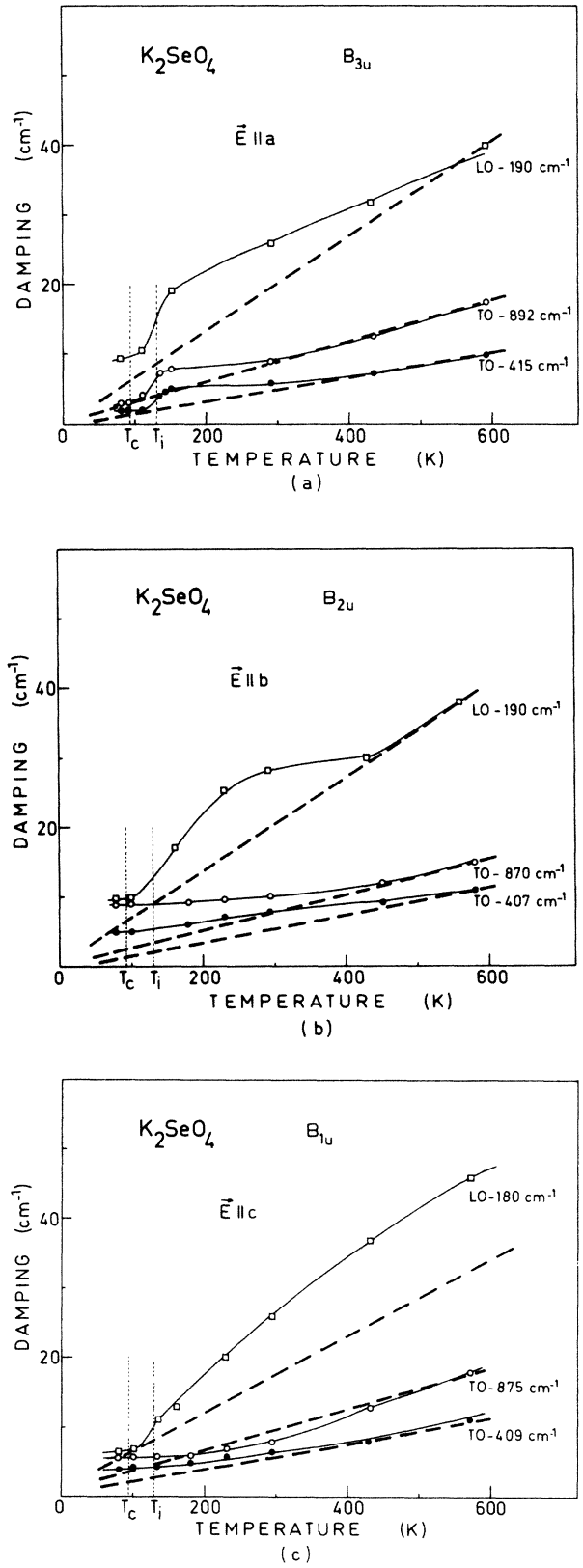

FIG. 8. Temperature dependence of LO phonon damping of main external mode and TO-phonon damping of main ν_3 and ν_4 modes for (a) **E**||**a**, (b) **E**||**b**, and (c) **E**||**c**. Dashed lines are results of Eq. (7); solid lines are guides to eye.

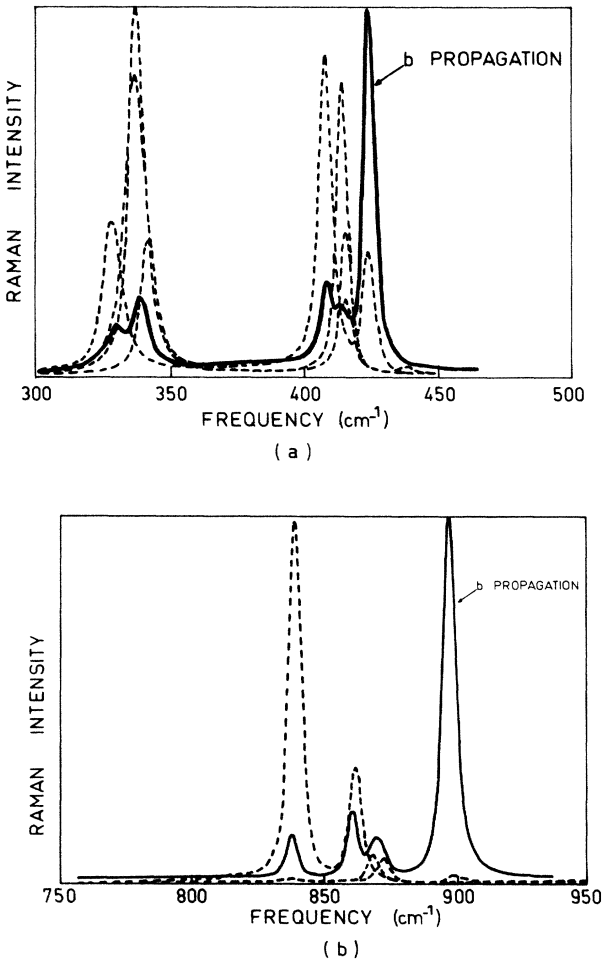

FIG. 9. Internal-mode Raman-scattering spectra for phonon propagation along the **b** orthorhombic axis at room temperature (see also Ref. 26). (a) bending-mode region and (b) stretching-mode region.

polarization wave. The lock-in leads to a flipping of local polarizations to give rise to a macroscopic spontaneous polarization. Then δ goes discontinuously to zero and the incommensurability is abruptly suppressed. There is, therefore, no "natural" lock-in with δ attaining continuously zero. A consequence of this fact is that defects or impurities can play an important role at the lock-in transition.[35,36] The domain or soliton density will vanish at some temperature lower than T_C when the intersoliton distance becomes too large. Summarizing, according to Bruce *et al.*,[37] the INC-COM transition is best regarded as an instability of the lattice against the creation of solitons.

The soliton density may be probed by magnetic resonance studies.[38] Blinc *et al.*[35,39] have worked on Rb_2ZnCl_4 between T_I and T_C. In their more recent paper,[35] they conclude that the plane-wave regime (where the phase is a linear function and the soliton density equal to 1) breaks down very close to T_I. However, if we com-

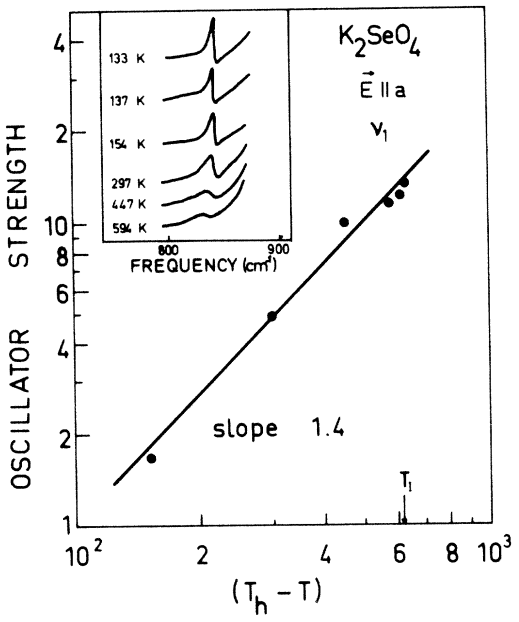

FIG. 10. Temperature dependence of TO oscillator strength of ν_1 mode in the PE phase. The evolution of infrared reflectivity of this mode is shown in the insert.

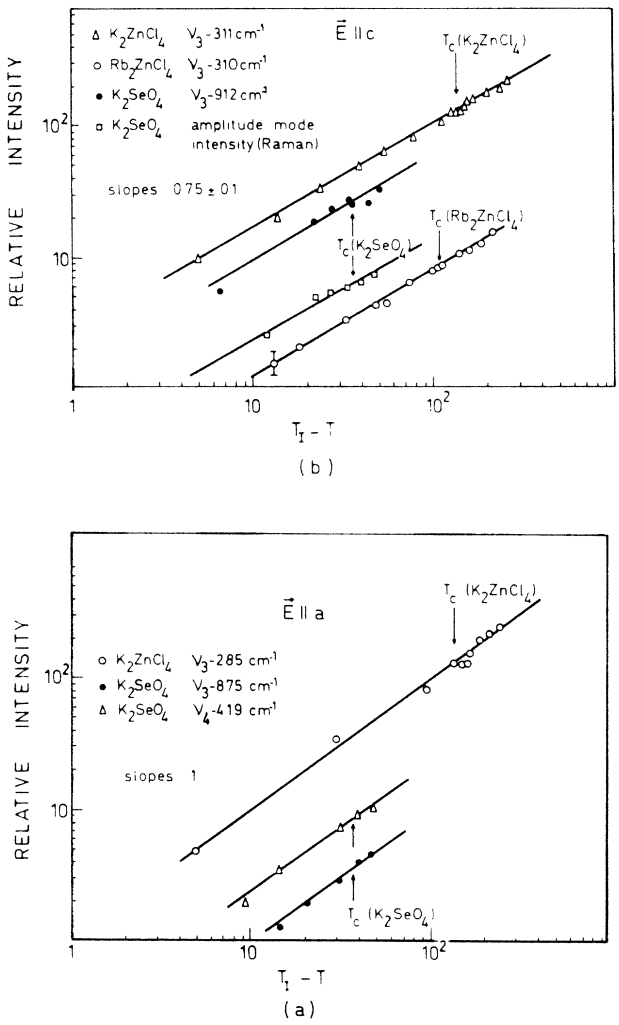

FIG. 11. Temperature dependence of the oscillator strengths of main additional TO modes in the INC and FE phases of K_2SeO_4. The behaviors of the amplitude-mode intensity and of oscillator strengths of additional modes of K_2ZnCl_4 and Rb_2ZnCl_4 are also shown for comparison. (a) **E**||**a** and (b) **E**||**c**.

pile the sequence of papers by Blinc *et al.*, it appears that the change of regime is sample dependent.[35,39,40] Conversely, Natterman[41] theoretically predicts that the soliton density remains equal to unity down to the critical region close to T_C in the absence of impurities. Defects in this class of phenomena appear, therefore, so important that it appears highly desirable to state precisely what is the role played by intrinsic defects such as isotopes. Concerning extrinsic defects, dielectric and differential thermal analysis studies[42] on Rb_2ZnCl_4 show considerable thermal hystereses from sample to sample. In some samples, T_C is not even observed, and one may wonder whether, in that case, the lock-in would be reached with δ varying continuously to zero on cooling so that the commensurate phase structure would be only a tripling of D_{2h} unit cell and no FE distortion would occur. No such sample-dependent phenomena were reported however for potassium selenate. It is important to notice that in a nonpolar INC compound such as Na_2CO_3,[43] where, therefore, the phenomenon of polarization wave does not occur, δ is found to reach zero continuously and the lock-in is a second-order phase transition.

ACKNOWLEDGMENTS

Part of this work was done while one of us (N.E.M.) was at Instituto de Fisica "Gleb Wataghin," Universidade Estadual de Campinas, 13100 Campinas, São Paulo, Brazil.

[1]M. Wada, A. Sawada, Y. Ishibashi, and Y. Takagi, J. Phys. Soc. Jpn. **42**, 1229 (1977).

[2]P. Echegut, F. Gervais, and N. E. Massa, Phys. Rev. B **31**, 581 (1985), and references therein.

[3]N. E. Massa, F. G. Ullman, and J. R. Hardy, Phys. Rev. B **27**, 1523 (1983).

[4]M. Iizumi, J. D. Axe, G. Shirane, and K. Shimaoka, Phys. Rev. B **15**, 4392 (1977).

[5]J. D. Axe, M. Iizumi, and G. Shirane, Phys. Rev. B **22**, 3408 (1980).

[6]J. Petzelt, G. V. Kozlov, A. A. Volkov, and Y. Ishibashi, Z. Phys. B **33**, 369 (1979).

[7]K. Inoue, K. Suzuki, A. Sawada, Y. Ishibashi, and Y. Takagi, J. Phys. Soc. Jpn. **46**, 608 (1979).
[8]G. Gattow, Acta Cryst. **15**, 419 (1962); A. Kalman, J. S. Stephens, and D. W. J. Cruickshank, Acta Cryst. B **26**, 1451 (1970).
[9]K. Aiki, K. Hukada, and O. Matamura, J. Phys. Soc. Jpn. **26**, 1066 (1969).
[10]P. M. de Wolff, Acta Cryst. A **33**, 493 (1977).
[11]A. Janner and T. Janssen, Phys. Rev. B **15**, 643 (1977); Acta Cryst. A **36**, 399 (1980); **36**, 408 (1980).
[12]T. Rasing, P. Wyder, A. Janner, and T. Janssen, Solid State Commun. **41**, 715 (1982); Phys. Rev. B **25**, 7504 (1982).
[13]V. A. Golovko and A. P. Levanyuk, Zh. Eksp. Teor. Fiz. **81**, 2296 (1981) [Sov. Phys.—JETP **54**, 1217 (1981)]; also in *Light Scattering Near Phase Transitions,* edited by H. Z. Cummins and A. P. Levanyuk (North-Holland, Amsterdam, 1983), Chap. 3, p. 169.
[14]H. Poulet and R. M. Pick, J. Phys. C **14**, 2675 (1981).
[15]A. Sawada, Y. Makita, and Y. Takagi, J. Phys. Soc. Jpn. **41**, 174 (1974).
[16]S. Shiozaki, A. Sawada, Y. Ishibashi, and Y. Takagi, J. Phys. Soc. Jpn. **43**, 1314 (1977).
[17]H. Arnold, W. Kurtz, A. Richler-Zinnius, and J. Bethke, Acta Cryst. B **37**, 1643 (1981).
[18]F. Gervais, in *Infrared and Millimeter Waves,* edited by K. J. Kutton (Academic, New York, 1983), Vol. 8, Chap. 7.
[19]H. G. Unruh, W. Eller, and G. Kirf, Phys. Status Solidi A **55**, 173 (1979).
[20]K. Aiki, K. Hukuda, H. Koga, and T. Kobayashi, J. Phys. Soc. Jpn. **28**, 389 (1970); S. Kudo and T. Ikeda, *ibid.* **50**, 733 (1981).
[21]J. F. Scott, Phys. Rev. B **4**, 1360 (1971).
[22]F. Gervais, Solid State Commun. **18**, 191 (1976); F. Gervais and H. Arend, Z. Phys. B **50**, 17 (1983).
[23]J. Petzelt, Phase Transitions **2**, 155 (1981), and references therein.
[24]N. E. Massa, P. Echegut, and F. Gervais, Ferroelectrics **53**, 281 (1984).
[25]S. Pacesova, B. Brezina, and L. Jastrabik, Phys. Status Solidi B **116**, 645 (1983).
[26]N. E. Massa and R. D. Kirby, in *Raman Spectroscopy-Linear and Nonlinear,* edited by J. Lascombe and P. Huong (Wiley, New York, 1982), p. 399.
[27]H. Bilz, H. Büttner, A. Bussman-Holder, W. Kress, and U. Schröder, Phys. Rev. Lett. **48**, 264 (1982).
[28]G. Pannetier and M. Gaultier, Bull. Soc. Chim. Fr. **1069**, 188 (1966).
[29]T. Watanabe, K. Sakai, and S. Iwai, Acta Cryst. A **28**, 187 (1972).
[30]M. Ishigame and S. Yamashita, Phys. Status Solidi B **116**, 49 (1983).
[31]H. Arnold, W. Kurtz, and H. Grimm, Ferroelectrics **25**, 557 (1980).
[32]P. Echégut, F. Gervais, and N. E. Massa, Phys. Rev. B **30**, 6039 (1984).
[33]S. Shiozaki, A. Sawada, Y. Ishibashi, and Y. Takagi, J. Phys. Soc. Jpn. **42**, 353 (1977).
[34]C. F. Majkrzak, J. D. Axe, and A. D. Bruce, Phys. Rev. B **22**, 5278 (1980).
[35]R. Blinc, B. Lozar, F. Milia, and R. Kind, J. Phys. C **17**, 241 (1984), and references therein.
[36]H. G. Unruh, J. Phys. C **16**, 3245 (1983).
[37]A. D. Bruce, in *Solitons and Condensed Matter Physics,* edited by A. R. Bishop and T. Schneider (Springer-Verlag, Berlin, 1978), p. 116; A. D. Bruce, R. A. Cowley, and A. F. Murray, J. Phys. C **11**, 3591 (1978).
[38]R. Blinc, Phys. Rep. **79**, 331 (1981).
[39]R. Blinc, I. P. Aleksandrova, A. S. Chaves, F. Milia, V. Rutar, J. Seliger, B. Topic, and S. Zumer, J. Phys. C **15**, 547 (1982).
[40]R. Blinc, Phys. Scr. **T1**, 138 (1982).
[41]T. Natterman, J. Phys. C **16**, 4113 (1983).
[42]M. Fahli, G. Godefroy, M. Jannin, B. Jannot, C. Dumas, and H. Arend, Ferroelectrics **53**, 251 (1984).
[43]E. Brouns, J. W. Wisser, and P. M. de Wolff, Acta Cryst. **17** 614 (1964); C. J. de Pater and R. B. Helmholdt, Phys. Rev. B **19**, 4684 (1979).